DOI: 10.1002/((please add manuscript number))

Article type: Communication

Entropy-Maximized Synthesis of Multi-Metallic Nanoparticle Catalysts via a Ultrasonication-Assisted Wet Chemistry Method under Ambient Conditions

Miaomiao Liu, Zihao Zhang, Francis Okejiri, Shize Yang, Shenghu Zhou* and Sheng Dai**

M. Liu, Prof. S. Zhou

School of Chemical Engineering, East China University of Science and Technology

Shanghai 200237, China

E-mail: zhoushenghu@ecust.edu.cn

M. Liu, Z. Zhang, F. Okejiri, Prof. S. Dai

Department of Chemistry, The University of Tennessee, Knoxville

Knoxville, TN 37996, USA

E-mail: dais@ornl.gov

Dr. S. Yang

Center for Functional Nanomaterials, Brookhaven National Laboratory

Upton, New York 11973, USA

E-mail: shize@bnl.gov

Prof. S. Dai

Chemical Sciences Division

Oak Ridge National Laboratory

Oak Ridge, TN 37831, USA

Keywords: ultrasonication-assisted, wet chemistry method, high-entropy-alloy, nanoparticles, alkaline HER

A facile ultrasonication-assisted wet chemistry method for preparing multi-component alloy nanoparticles including high-entropy alloys is reported. PtAuPdRhRu alloy (high-entropy alloy), quaternary PtAuPdRh alloy and ternary PtAuPd alloy nanoparticles were produced with ~3 nm in diameter. Taking advantage of the acoustic cavitation phenomenon in ultrasonication process, noble metal precursors could be co-reduced by chemical reductants and transform to alloy structures under operation at room conditions. The instantaneous massive energy (~5000 °C, 2000 atm) occurring in momentary timespans ($\leq 10^{-9}$ s) contributes to the formation of multi-metallic mixed nanomaterials driven by entropy maximization. Owing to strong synergistic effects, the catalysts with the high-entropy-alloy nanoparticles supported on carbons exhibit prominent electrocatalytic activities for hydrogen evolution reaction.

Compared to their single component analogues, alloy materials demonstrate diverse mechanical and chemical properties such as lattice distance and electron distribution.[1,2] Because of these features, designing alloy structures with novel metallic combinations is a way to produce more functional materials. Among various alloy materials, high-entropy alloys (HEAs), has attracted increasing attention in many fields. Unlike common alloys not exceeding three elements, HEAs consist of five or more metallic elements with equiatomic or near equiatomic concentration, and these constituent atoms are uniformly dsitributed in a single-phase solid solution.[3,4] Owing to strong synergistic effects, HEAs illustrate excellent perfomances, such as mechnical hardness and

catalytic performances.[5,6] However, high temperature (> 900 °C) is usually required to generate high-entropy structures (ΔG = ΔH – TΔS). A widely reported approach for synthesizing multi-metallic alloy materials is to melt isolated single-metal solids into bulk alloys at high temperatures or pressures.[7-11] Such strict technical requirements in the synthetic process greatly limit the variety of alloys that can be created. Moreover, the melting method can hardly control the morphology of the products and meet the demand to bring these materials to nanoscale range. Consequently, alloying multi-metallic elements at the nanoscale is of critical importance, espically via the development of technologically feasible and facile methods.

Traditional alloy nanoparticles (NPs) are derived from the co-redcution of metallic ions by wet chemistry methods,[12-14] with help of chemical reductants and heating protocols at ≤ 300 °C.[15-17] The formation of alloy nanoparticles is mainly driven by enthapy interactions among metalic species, which is why most reported alloy NPs synthesized by traditional wet chemistry methods have not exceeded three different metals. Several studies have emerged detailing the production of multi-metallic alloy NPs, especially high-entropy-alloy (HEA) NPs under high temperature conditions. Notably, Yao *et* al. synthesized HEA-NPs (≥ 5 nm) by a two-step carbothermal shock method.[18] This strategy employed flash heating and cooling, where an extremely high temperature (~2000 K) was applied for a momentary timespan (~55 ms). They conclude that one determining condition for forming HEA-NPs is a sharp temperature ramp rate that maximizes the entropic factor in controlling final products.[18]

In an ultrasound irradiation process, the acoustic cavitation phenomenon can generate extremely high temperatures in localized microscopic regions at momentary timespans, thereby meeting one of the conditions presented by Yao *et* al.[18] The acoustic cavitation phenomenon can

be described as the formation, successive growth and implosive collapse of microscopic bubbles. The collapse of those bubbles generates pressure of ~2000 atm and temperatures of ~5000 °C in localized microscopic regions at a timescale of ≤ 10^{-9} s.[19,20] This instantaneous release of massive energy can accelerate reactant molecules and drive product growth to entropy-maximized states.[21,22] With the help of ultasonication, it is possible to generate Fe/Co alloy NPs at room temperature.[23] Under a 40 kHz ultrasonic wave, ethylene glycol reduces Pd^{2+} and Au^{3+} ions to PdAu bimetallic alloys at room temperature.[24] Rationally, an ultrasonication-assisted wet chemistry method is a promising strategy for producing HEA-NPs. In the absence of reported works, the studies presented herein verify the feasibility of synthesizing multi-metallic alloy NPs via this method. Under intense ultrasonication irradiation, Pt^{4+}, Au^{3+}, Pd^{2+}, Rh^{3+} and Ru^{3+} ions were co-reduced under ambient conditions in a few minutes with ethylene glycol functioning as both the reductant and solvent. Using this technique, ternary PtAuPd, quaternary PtAuPdRh, and quinary PtAuPdRhRu alloy NPs (HEA-NPs) were all successfully synthesized. More importantly, a very small particle size (~3 nm) was achieved in the rapid reduction process and absence of high-temperature reduction conditions.

Electrochemical water splitting is an emerging technology for energy conversion, which is broken down into the cathodic hydrogen evolution reaction (HER) and the anodic oxygen evolution revolution reaction (OER).[25,26] As discussed in recent papers, the HER catalytic activity in alkaline solutions is more difficult than in acidic solution, which is ascribed to weaker H/OH-binding and a higher energy barrier for water dissociation on the catalyst surface.[27,28] Modulating the electronic and geometric structures of the catalysts is a workable strategy to enhance HER catalytic perfomance, as seen from the results of various shape-controlled bimetallic nanocatalysts.[29-33] The synergistic effects of the different metals in multi-metallic catalysts generally exhibit enhanced

performance than monometallic materials in electrocatalytic reactions. The electrocatalytic activities of as-synthesized alloy materials were tested and presented satisfactory results for HER.

For synthesizing the HEA quinary NPs, equimolar amounts of K_2PdCl_4, $HAuCl_4$, H_2PtCl_6, $RuCl_3$ and $RhCl_3$ were dissolved in ethylene glycol followed by adding a calculated amount of X-72 carbon support for a total noble metallic weight loading of 10 %. As presented in **Scheme 1**, the mixture was placed in an ultrasonication processor and exposed to intense radiation. A cylindrical tip was introduced into the liquid to perform ultrasonication working at 750 watts and 20 kHz at ambient conditions for 10 minutes. Subsequently, the amorphous HEA-NPs supported on carbon structures were obtained through filtration. To obtain stable HEA-NPs/carbon nanocatalysts, the resulting solids were calcined under N_2 at 500 or 700 °C for 2h. Both PtAuPd ternary and PtAuPdRh quaternary structures were synthesized through a similar process.

X-ray diffraction (XRD) patterns of a series of as-synthesized alloy materials are presented in **Figure 1**. The HEA-NPs/carbon produced from 10 min of the ultrasonication-assisted wet chemistry method (**Figure 1a**) displays an additional set of FCC diffraction patterns. This phenomenon demonstrates a two-phase microstructure.[3] As presented in **Figures 1b and 1c**, the shoulder peaks decrease for HEA-NPs/carbon-500 °C and disappear totally for HEA-NPs/carbon-700 °C. The XRD patterns of HEA-NPs/carbon-700 °C exhibit only one set of diffraction peaks for FCC structure. Combining XRD results with STEM mapping in **Figure 2**, the alloy structures of HEA-NPs/carbon-700 °C are confirmed. Consequently, calcination at high temperature would maturate the alloy structures. Through the ultrasonication-assisted wet chemistry method, ternary and quaternary multi-metal-alloy NPs were also produced. XRD patterns for PtAuPdRh/carbon-700 °C and PtAuPd/carbon-700 °C are shown in **Figure 1d and 1e**. Interestingly, ternary NPs still display an

additional FCC phase after calcination, while quaternary NPs present a tiny additional phase. As reported, the higher entropy of elements in nanoscale systems contribute to increased tendency of uniform phase.[34,35] Therefore, it is reasonable to posit that increasing the variety of different metals accelerates the alloying process to a certain extent.

Figures 2 and S2 display the particle morphologies and elemental distributions of HEA-NPs/carbon-700 °C and HEA-NPs/carbon materials. The uniform distribution of Pt, Au, Pd, Rh and Ru in the nanospheres certify the formation of an alloy structure directly. Energy dispersive X-ray spectroscopy (EDS) data additionally corroborates this assertion with the signal intensity for all elements presented in **Figure S1**. The elemental distribution of HEA-NPs/carbon in **Figure S2** shows that none of the metals are preferentially situated in different particles before calcination, they are present throughout these nanoparticles further corroborating the formation of an alloy structure using the ultrasonication-assisted wet chemistry method. Comparing the elemental distribution of the HEA-NPs/carbon before and after calcination further strengthens the assertion that the calcination process generates an alloy structure supported over the carbon. **Figure 3** shows the elemental distribution on the ternary and quaternary NPs after calcination in the PtAuPdRh/carbon-700 °C and PtAuPd/carbon-700 °C, respectively. The results are analogous to those for HEA-NPs/carbon-700 °C: all metallic elements distribute uniformly within the nanosphere (~3 nm), indicating an alloy structure. This demonstrates that the ultrasonication-assisted wet chemistry method is a feasible and universal way to synthesize various proportions of multi-metal-alloy NPs. Additionally, the morphology of the materials does not change significantly after calcination. **Figure 2a and 2b** show the average particle size distribution for both the uncalcined HEA-NPs/carbon and HEA-NPs/carbon-700 °C. Their average diameters are 2.8 ± 0.3 nm and 2.6 ± 0.3 nm respectively.

These results demonstrate that calcination under an N_2 atmosphere matures the alloy structures but does not appreciably enlarge their size, from which we can infer that these HEA structures have superior stability at high temperatures.

The electrocatalytic HER performances of as-synthesized multi-metallic-alloy nanocatalysts were assessed in a three-electrode system using an aqueous 1.0 M KOH solution as the electrolyte. Polarization curves for HER and Tafel plots of HEA-NPs/carbon-700 °C, PtAuPdRh/carbon-700 °C, PtAuPd/carbon-700 °C and commercial Pt/C (Pt weight loading - 20%) catalysts are presented in **Figure 4**. The Tafel plots of potential – log |current density| show a single slope line that can be attributed to the well-known two-step Volmer-Tafel mechanism for HER.[36] Accordingly, the HER kinetics in alkaline solutions for the Volmer-Tafel mechanism involves two steps: an electron-coupled water dissociation forming adsorbed hydrogen (Volmer step); and the subsequent combination of the adsorbed hydrogen into H_2 (Tafel step). In alkaline solutions, lower HER activities generally result from the sluggish Volmer step.[37] The value of the Tafel slope reflects the kinetic mechanism for HER. Smaller Tafel slopes demonstrated a lower energy barrier of Volmer step and an accelerated Volmer step for HER.[38] Thermogravimetric analysis measurement (**Figure S3**) was exerted to estimate the loading amount of active metal on carbon support, as discussed in SI (*Electrocatalytic HER performance test*). Owing to metallic ions reduced totally, the loading weight of whole noble metals was estimated to 10 % wt and the loading amount of total noble metal on the electrode is 0.03 mg cm^{-2} depending on the presursors amount.

As shown in **Figure 4a**, these multi-metallic catalysts all perform well for the HER, while HEA-NPs/carbon-700 °C displays excellent electrocatalytic activity. For HEA-NPs/carbon-700 °C, the onset potential of the HER is –0.025 V vs. RHE and the current density reach 30 mA cm^{-2} at a potential of –

0.19 V vs. RHE. PtAuPdRh/carbon-700 °C and PtAuPd/carbon-700 °C present similar onset potentials near 0 V vs. RHE but reach current densities of 30 mA cm^{-2} at –0.26 V vs. RHE and –0.6 V vs. RHE, respectively. Under the same test conditions, the commercial Pt/C catalyst shows reduced electrocatalytic performance relative to HEA-NPs/carbon-700 °C, but similar to quaternary PtAuPdRh/carbon-700 °C. In **Figure 4b**, HEA-NPs/carbon-700 °C exhibits a Tafel slope value of 62 mV $dec.^{-1}$, which is smaller than commercial Pt/C (77 mV $dec.^{-1}$), PtAuPdRh/carbon-700 °C (91 mV $dec.^{-1}$) and PtAuPd/carbon-700 °C (177 mV $dec.^{-1}$). With less than 0.03 mg cm^{-2} loading of active metal, the operating potential –0.37 V to deliver 100 mA cm^{-2} is better than several noble metallic electrocatalysts yet reported.[32,33] As compared, Pt catalysts are measured with a Tafel slope of 116 mV $dec.^{-1}$ in alkaline solution (0.1 M NaOH).[39] Ru nanomaterials presents a Tafel slope of 118 mV $dec.^{-1}$ in 0.1 M KOH.[38] The small slope of 62 mV $dec.^{-1}$ demonstrates small energy barrier of Volmer step and a fast Tafel step-determined HER process. To test the stability of the as-synthesized HEA-NPs/carbon-700 °C catalysts, chronopotentiometry curve at 100 mA cm^{-2} was obtained (**Figure S4**). The HEA-NPs/carbon-700 °C shows stable electrocatalytic performance over an 8 h period. The superior electrocatalytic performance of HEA-NPs/carbon-700 °C is ascribed to strong synergistic effects resulting from different metallic atoms.[40,41] With different element adding comes with improved entropy of the alloy system. An entropy-maximized alloy system would demonstrate maximized synergistic effects, hence improves catalytic performance.[42]

Unlike traditional wet chemistry methods, this work takes advantage of ultrasonication to produce multi-metallic alloy NPs with diameters of less than 3 nm. The acoustic cavitation generated during the ultrasonication process has the potentials of generating instantaneously massive energy in momentary timespans, which can be used to facilitate the formation of alloyed products. Through

this ultrasonication-assisted wet chemistry method, quinary PtAuPdRhRu-NPs (HEA-NPs), quarternary PtAuPdRh-NPs and ternary PtAuPd-NPs were produced and suppored on XC-72 carbon in a one-step process. For HER, HEA-NPs/carbon materials present prominent onset potential at –0.025 V vs. RHE, and a remarkable Tafel slope in alkaline environment. Enhanced elctrocatalytic activities are ascribed to high-entropy at nanoscale and strong synergistic effects between active metals. This is a technologically feasible and facile strategy for producing HEA-NPs that does not ascribe to the limitations in metal selection that other wet chemistry methods suffer from and, as such, is highly instructive for creating a significantly wider variety of alloy nanoparticles.

Supporting Information

Supporting Information is available from the Wiley Online Library or from the author.

Acknowledgements

The research was supported by the U.S. Department of Energy, Basic Energy Science, Chemical, Geoscience, and Bioscience Division. Part pf the electron microscopy analysis was carried out at the Centre for Functional Nanomaterials, Brookhaven National Laboratory (BNL), which is supported by the DOE, Office of Basic Energy Science, under contract DE-SC0012704. S. Zhou thanks the National Natural Science Foundation of China (Grant No. 21776090). M. Liu was financially supported by the China Scholarship Council for 1 year's study at the University of Tennessee and Oak Ridge National Laboratory.

Received: ((will be filled in by the editorial staff))
Revised: ((will be filled in by the editorial staff))
Published online: ((will be filled in by the editorial staff))

References

[1] J. Freudenberger, D. Rafaja, D. Geissler, L. Giebeler, C. Ullrich, A. Kauffmann, M. Heilmaier, K. Nielsch, *Metals* **2017**, *7*, 135.

[2] H. Zhang, L. Lu, Y. Cao, S. Du, Z. Cheng, S. Zhang, *Mater. Res. Bull.* **2014**, *49*, 393.

[3] S. Sohn, Y. Liu, J. Liu, P. Gong, S. Prades-Rodel, A. Blatter, B.E. Scanley, C.C. Broadbridge, J. Schroers, *Scripta Mater.* **2017**, *126*, 29.

[4] Y. Zhang, T. Zuo, Z. Tang, M. Gao, K. A. Dahmen, P. K. Liaw, Z. Lu, *Prog. Mater. Sci.* **2014**, *61*, 1.

[5] T. Jin, X. Sang, R. R. Unocic, R. T. Kinch, X. Liu, J. Hu, H. Liu, S. Dai, *Adv. Mater.* **2018**, *30*, 1707512.

[6] J. W. Yeh, S. Chen, S. Lin, J. Gan, T. S. Chin, T. Shun, C. H. Tsau, S. Chang, *Adv. Eng. Mater.* **2004**, *6*, 299.

[7] J. Cieslak, J. Tobola, K. Berent, M. Marciszko, *J. Alloy. Compd.* **2018**, *740*, 264.

[8] C. C. Tung, J. W. Yeh, T. Shun, S. Chen, Y. Huang, H. Chen, *Mater. Lett.* **2007**, *61*, 1.

[9] Y. Wang, B. Li, M. Ren, C. Yang, H. Fu, *Mater. Sci. Eng. A* **2008**, *491*, 154.

[10] S. Susarla, A. Kutana, J. A. Hachtel, V. Kochat, A. Apte, R. Vajtai, J. C. Idrobo, B. I. Yakobson, C. S. Tiwary, P. M. Ajayan, *Adv. Mater.* **2017**, *29*, 1702457.

[11] B. Gurau, R. Viswanathan, R. Liu, T. J. Lafrenz, K. L. Ley, E. S. Smotkin, E. Reddington, A. Sapienza, B. Chan, T. E. Mallouk, S. Sarangapani, *J. Phys. Chem. B* **1998**, *102*, 9997.

[12] S. Zhou, G. S. Jackson, B. Eichhorn, *Adv. Funct. Mater.* **2007**, *17*, 3099.

[13] S. Mourdikoudis, L. M. Liz-Marzán, *Chem. Mater.* **2013**, *25*, 1465.

[14] S. Alayoglu, B. Eichhorn, *J. Am. Chem. Soc.* **2008**, *130*, 17479.

[15] D. Lu, Y. Zhang, S. Lin, L. Wang, C. Wang, *Talanta* **2013**, *112*, 111.

[16] F. Bonet, V. Delmas, S. Grugeon, R. Herrera Urbina, P.Y. Silvert, K. Tekaia-Elhsissen, *Nanostruct. Mater.* **1999**, *11*, 1277.

[17] K. Patel, S. Kapoor, D. P. Dave, T. Mukherjee, *J. Chem. Sci.* **2005**, *117*, 311.

[18] Y. Yao, Z. Huang, P. Xie, S. D. Lacey, R. J. Jacob, H. Xie, F. Chen, A. Nie, T. Pu, M. Rehwoldt, D. Yu, M.R. Zachariah, C. Wang, R. Shahbazian-Yassar, J. Li, L. Hu, *Science* **2018**, *359*, 1489.

[19] A. Moghtada, R. Ashiri, *Ultrason. Sonochem.* **2018**, *41*, 127.

[20] A. Gedanken, *Ultrason. Sonochem.* **2004**, *11*, 47.

[21] A. Moghtada, R. Ashiri, *Ultrason. Sonochem.* **2016**, *33*, 141.

[22] A. Moghtada, A. Shahrouzianfar, R. Ashiri, *Adv. Powder Technol.* **2017**, *28*, 1109.

[23] Q. Li, H. Li, V. G. Pol, I. Bruckental, Y. Koltypin, J. Calderon-Moreno, I. Nowik, A. Gedanken, *New J. Chem.* **2003**, *27*, 1194.

[24] K. Canxia, C. Weiping, L. Cuncheng, Z. Lide, H. Hofmeister, *J. Phys. D: Appl. Phys.* **2003**, *36*, 1609.

[25] C. C. L. McCrory, S. Jung, I. M. Ferrer, S. M. Chatman, J. C. Peters, T. F. Jaramillo, *J. Am. Chem. Soc.* **2015**, *137*, 4347.

[26] M. Zeng, Y. Li, *J. Mater. Chem. A* **2015**, *3*, 14942.

[27] Y. Zheng, Y. Jiao, A. Vasileff, S. Qiao, *Angew. Chem., Int. Ed.* **2018**, *57*, 7568.

[28] N. Mahmood, Y. Yao, J. Zhang, L. Pan, X. Zhang, J. Zou, *Adv. Sci.* **2018**, *5*, 1700464.

[29] C. W. Lee, K. D. Yang, D.-H. Nam, J. H. Jang, N. H. Cho, S. W. Im, K. T. Nam, *Adv. Mater. 0*, 1704717.

[30] V. R. Stamenkovic, B. S. Mun, M. Arenz, K. J. J. Mayrhofer, C. A. Lucas, G. Wang, P. N. Ross, N. M. Markovic, *Nat. Mater.* **2007**, *6*, 241.

[31] J. Greeley, I. E. L. Stephens, A. S. Bondarenko, T. P. Johansson, H. A. Hansen, T. F. Jaramillo, J. Rossmeisl, I. Chorkendorff, J. K. Nørskov, *Nat. Chem.* **2009**, *1*, 552.

[32] H. Yin, S. Zhao, K. Zhao, A. Muqsit, H. Tang, L. Chang, H. Zhao, Y. Gao, Z. Tang, *Nat. Comm.* **2015**, *6*, 6430.

[33] X. Zhong, Y. Qin, X. Chen, W. Xu, G. Zhuang, X. Li, J. Wang, *Carbon* **2017**, *114*, 740.

[34] H. Y. Diao, R. Feng, K. A. Dahmen, P. K. Liaw, *Curr. Opin. Solid St. M.* **2017**, *21*, 252.

[35] D. B. Miracle, O. N. Senkov, *Acta Mater.* **2017**, *122*, 448.

[36] J. Zhang, T. Wang, P. Liu, Z. Liao, S. Liu, X. Zhuang, M. Chen, E. Zschech, X. Feng, *Nat. Comm.* **2017**, *8*, 15437.

[37] F. Safizadeh, E. Ghali, G. Houlachi, *Int. J. Hydrogen Energ.* **2015**, *40*, 256.

[38] N. Danilovic, R. Subbaraman, D. Strmcnik, K. Chang, A. P. Paulikas, V. R. Stamenkovic, N. M. Markovic, *Angew. Chem., Int. Ed.* **2012**, *124*, 12663.

[39] I. Ledezma-Yanez, W. D. Z. Wallace, P. Sebastián-Pascual, V. Climent, J. M. Feliu, M. T. M. Koper, *Nat. Energ.* **2017**, *2*, 17031.

[40] Z. Xia, P. Zhang, G. Feng, D. Xia, J. Zhang, *Adv. Mater. Interfaces* 2018, 5, 1800297.

[41] J. Wang, J. Chen, J. Chen, H. Zhu, M. Zhang, M. Du, *Adv. Mater. Interfaces* 2017, 4, 1700005.

[42] H. Chen, J. Fu, P. Zhang, H. Peng, C. Abney, K. Jie, X. Liu, M. Chi, S. Dai, *J. Mater. Chem. A* 2018, 6, 11129-11133.

Scheme 1. Schematic illustration of synthesis of HEA-NPs/carbon (PtAuPdRhRu supported on XC-72 carbon) catalysts and their application in hydrogen evolution reactions.

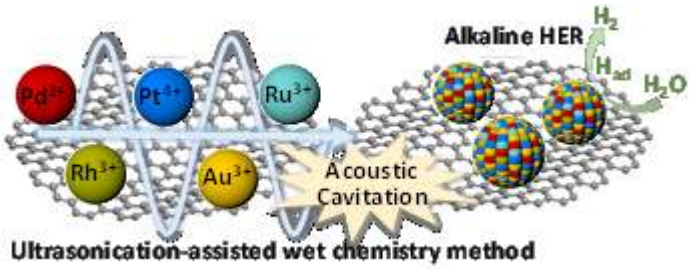

Figure 1. XRD patterns of HEA-NPs/carbon synthesized from (a) ultrasonication-assisted wet chemistry method, followed by calcination under N_2 at (b) 500 °C and (c) 700 °C for 2h, (d) PtAuPdRh/carbon and (e) PtAuPd/carbon synthesized from ultrasonication-assisted wet chemistry method and calcination under N_2 at 700 °C for 2h.

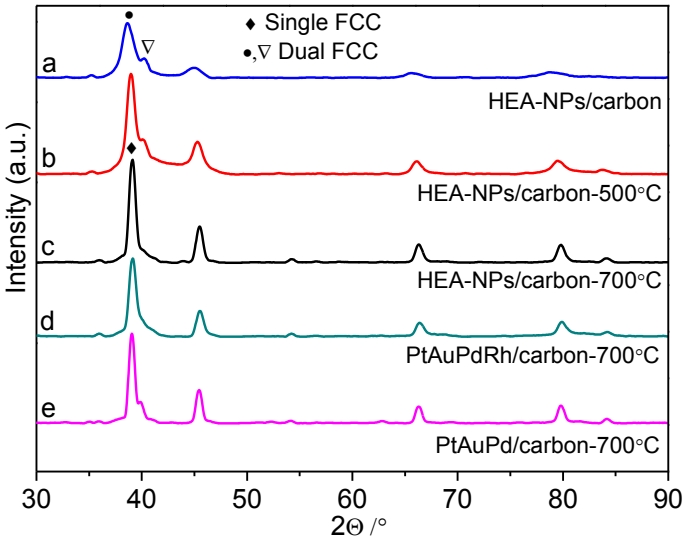

Figure 2. STEM image of (a) HEA-NPs/carbon and (b) HEA-NPs/carbon-700 °C. HAADF image and EDS elemental maps of mixed (c), Pt (d), Au (e), Pd (f), Rh (g), and Ru (h) for HEA-NPs/carbon-700 °C (selected area in Figure 2b inset). Particle size analyses of HEA-NPs/carbon (inset in a) and HEA-NPs/carbon-700 °C (inset in b).

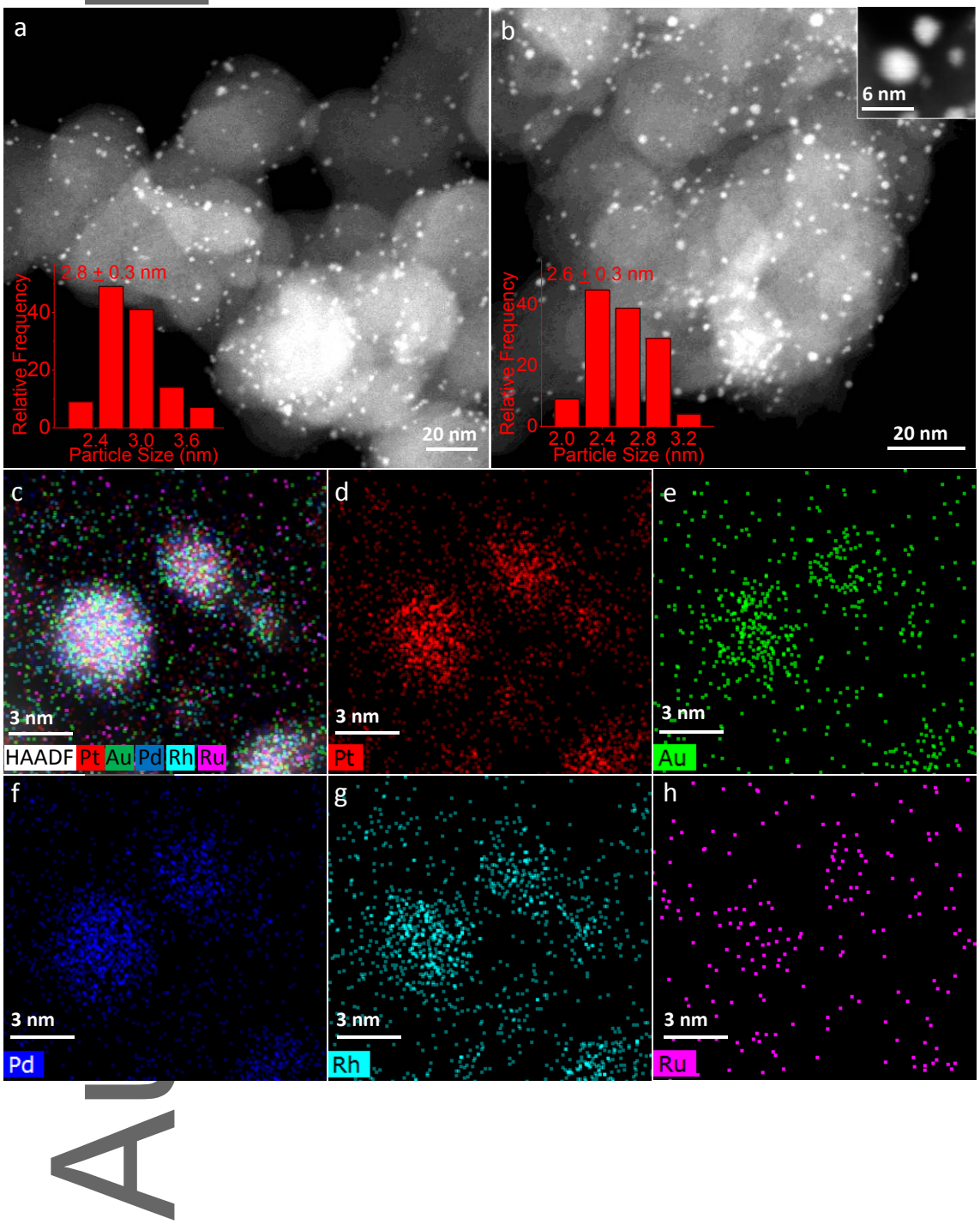

Figure 3. HAADF image and EDS elemental maps of a-e) for PtAuPdRh-NPs/carbon-700 °C and f-g) for PtAuPd-NPs/carbon-700 °C.

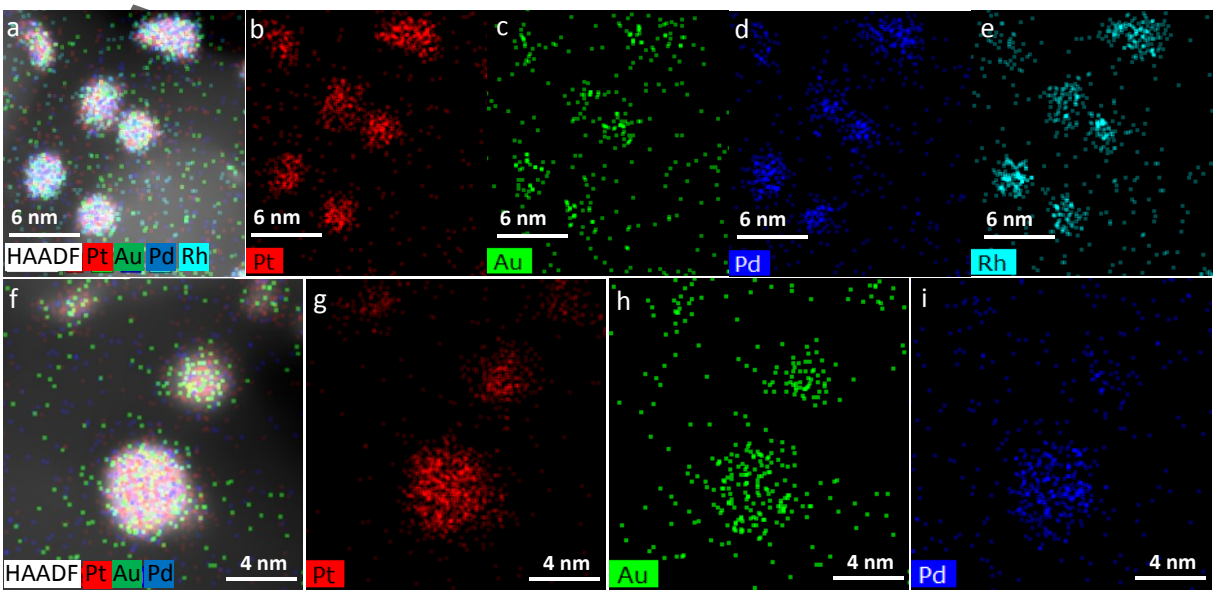

Figure 4. (a) Polarization curves and (b) Tafel plots of HEA-NPs/carbon-700 °C, PtAuPdRh/carbon-700 °C, PtAuPd/carbon-700 °C and commercial Pt/C (Pt loading – 20 wt%) catalysts in 1.0 M KOH.

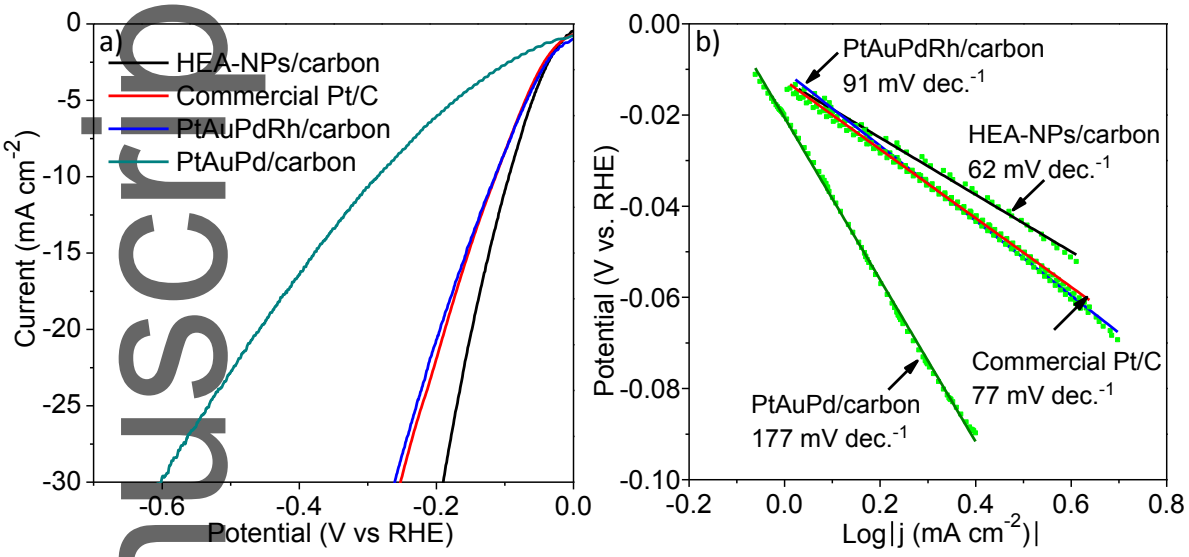

Taking advantages of the acoustic cavitation phenomenon in ultrasonic irraditions process, an ultrasonication-assisted wet chemistry method is designed to alloy multimetallic elements in nanoscales. Quinary PtAuPdRhRu (High-entropy-alloy), quaternary PtAuPdRh and ternary PtAuPd nanoparticles were synthesized with diameters of ~3 nm and supported on carbon in one step. The as-synthesized high-entropy-alloy materials present excellent electrocatalytic performance for alkaline HER.

ultrasonication-assisted, wet chemistry method, high-entropy-alloy, nanoparticles, alkaline HER

Miaomiao Liu, Zihao Zhang, Francis Okejiri, Shize Yang*, Shenghu Zhou* and Sheng Dai*

Entropy-Maximized Synthesis of Multi-Metallic Nanoparticle Catalysts via a Ultrasonication-Assisted Wet Chemistry Method under Ambient Condition